Preparation, Characterization, and Catalytic Properties for the SCR of NO by NH_3 of V_2O_5/TiO_2 Catalysts Prepared by Equilibrium Deposition Filtration

I. Georgiadou,[†] Ch. Papadopoulou,[†,‡] H. K. Matralis,[‡] G. A. Voyiatzis,[‡] A. Lycourghiotis,[†,‡] and Ch. Kordulis*[,†,‡]

Department of Chemistry, University of Patras, and Institute of Chemical Engineering and High-Temperature Chemical Processes, ICE/HT-FORTH, P.O. Box 1414, GR. 26 500, Patras, Greece

Received: September 30, 1997; In Final Form: March 15, 1998

V_2O_5/TiO_2 catalysts of varying vanadium content were prepared at various pH's and concentrations of the impregnation solution using the equilibrium deposition filtration (EDF) method. Moreover, corresponding catalysts were prepared using the conventional wet impregnation (WI) method. The above catalysts were exhaustively characterized using BET, AEM, FT-IR, DRS, LRM, XPS, TPR, and TPD of NH_3 and tested for the SCR of NO by NH_3 in the temperature range 250−450° C. It was found that the application of EDF results in V_2O_5/TiO_2 catalysts with relatively high dispersity of the vanadia supported phase, homogeneous distribution of this phase on the support particles, and quite strong interactions between the supported vanadia phase and the surface of titania, and inhibits the formation of supported V_2O_5 crystallites. The catalysts prepared by EDF exhibited better activity and selectivity than those prepared by conventional WI. Decrease of the impregnation pH in the EDF preparations from 8 to 4.5 caused an increase in the vanadium content from 2.6 to 3.6 wt % V_2O_5 which, in turn, provoked very important differences in the physicochemical properties of the EDF catalysts (increase of the surface coverage of the titania by the vanadia phase and decrease of the mean value of the vanadia phase−support interactions). The above explained the increase, with the vanadium content, of the activity and selectivity of the V_2O_5/TiO_2 EDF catalysts.

Introduction

The emission of NO from power plants causes very serious environmental problems. The most widely adopted process to destroy NO is its selective catalytic reduction (SCR) by ammonia over vanadia catalysts supported on titania. The effort has been mainly directed toward the investigation of the $V^{(v)}$ supported species responsible for catalytic activity and selectivity and to the elucidation of the whole catalytic cycle as well.[1−3] In most cases the related studies have been performed using V_2O_5/TiO_2 catalysts prepared by the conventional impregnation of anatase in electrolytic solutions containing $V^{(v)}$ species followed by drying and calcination.[4] The application of this method results in catalysts with larger supported crystallites weakly bounded on the support surface and complicated supported phases as compared to the corresponding catalysts prepared using the equilibrium deposition filtration (EDF) method, otherwise called "equilibrium adsorption". The identification, thus, of the supported V species responsible for the catalytic activity is quite difficult. In spite of this, studies on V_2O_5/TiO_2 catalysts prepared by EDF are not abundant in the literature.[5−10] Moreover, even in the studies on V_2O_5/TiO_2 catalysts prepared by EDF, the V species deposited, during impregnation, on the support surface were unknown, and some explanations developed were based on the V species present in the impregnation solution.[5] Recently,[11] the identification of the kind and the determination of the concentration of the V species deposited on the anatase surface have been achieved over a wide pH range and vanadium concentration using an advanced calculation procedure developed in the past years.[12−18]

The purpose of the present work is twofold: first, the comparison of the EDF catalysts with the corresponding ones prepared by the classical wet impregnation technique (WI); second, to study the influence of the preparation parameters, used in EDF, on the physicochemical and catalytic properties of the V_2O_5/TiO_2 catalysts.

Experimental Section

Catalysts Preparation. The titania support (anatase) was prepared by hydrolysis of titanium isopropoxide as described in detail previously.[19]

Two methods were followed for depositing the $V^{(v)}$ species on the surface of anatase: equilibrium deposition filtration (EDF) and the conventional wet impregnation technique (WI). Following EDF, an amount of anatase powder equal to 5 g was added in a NH_4VO_3 solution of 1.5×10^{-3} or 6×10^{-4} mol $V^{(v)}$ dm^{-3}, totaling 2.5 dm^3. In all cases the ionic strength of the solution was adjusted to 0.1 N using NH_4NO_3. Four catalysts were prepared using EDF at various pH's (4.5, 6.0, and 8.0). The pH of the suspension was regulated using HNO_3 or NH_4OH. In three cases the initial concentration of the impregnating solution was 1.5×10^{-3} mol $V^{(v)}$ dm^{-3}. This concentration corresponds to the plateau of the corresponding deposition isotherms presented previously.[11] In the fourth case the pH of the impregnating solution was 4.5, but its concentration was 6×10^{-4} mol $V^{(v)}$ dm^{-3}, representing thus the conditions that existed to a point of the rising part of the corresponding deposition isotherm.[11] This concentration was selected in order to obtain a catalyst with the same loading with

* To whom all correspondence should be addressed. Fax (+30-61) 994 796.

[†] Department of Chemistry, University of Patras.

[‡] Institute of Chemical Engineering and High Temperature Chemical Processes.

10.1021/jp973187y CCC: $15.00
Published on Web 10/06/1998

TABLE 1: V_2O_5/TiO_2 Catalysts Prepared Using Equilibrium Deposition Filtration (EDF) and Wet Impregnation (WI), the "V_2O_5" Content, the Values of the Impregnation Parameters, and the Specific Surface Area (SSA) of the Samples Determined after Calcination at 500 °C for 5 h

sample	% wt "V_2O_5"	pH	C_0[a]/ mol dm^{-3}	T/°C	SSA[b]/ m^2 g^{-1}
T-V(EDF)$_1$-2.6	2.6	8.0	1.5×10^{-3}	25	46 (47)
T-V(EDF)$_2$-2.6	2.6	4.5	6.0×10^{-4}	25	43 (44)
T-V(WI)-2.6	2.6				55 (56)
T-V(EDF)-3.4	3.4	6.0	1.5×10^{-3}	25	55 (57)
T-V(EDF)-3.6	3.6	4.5	1.5×10^{-3}	25	54 (56)
T-V(WI)-3.6	3.6				49 (51)
TiO_2 (anatase)	0.0				64

[a] Indicates the initial concentration of the impregnation solution used to prepare the EDF samples. [b] The numbers in parentheses indicate the SSA determined per gram of anatase.

that prepared at pH = 8.0 and initial solution concentration corresponding to the plateau of the corresponding deposition isotherm. After stirring for 20 h at 25° C, the suspension was filtered using membrane filters (Millipore, 0.22 μm). The resulting solid was dried at 120° C for 2.5 h, and then it was calcined at 500° C for 5 h. The $V^{(v)}$ content in the catalysts prepared was determined using UV−visible and atomic absorption spectroscopies.[20]

To investigate the influence of the preparation method on the physicochemical and catalytic properties of the V_2O_5/TiO_2 catalysts, two samples were prepared using the conventional wet impregnation technique. Following WI, an amount of $VO(C_2O_4)_2$ calculated to correspond to the desired amount of $V^{(v)}$ to be supported was dissolved in 100 cm^3 of bidistilled water. A 5 g sample of anatase was added, and the suspension was stirred for 1 h. Then the solvent was progressively evaporated using a rotary evaporator. The resulting solid was then dried and calcined as described above.

The catalysts prepared are presented in Table 1. It may be seen that, in the case of the EDF catalysts prepared using impregnation solution with constant concentration, the decrease in the pH of the solution causes an increase in the amount of $V^{(v)}$ deposited on the support surface.

Catalytic Tests. The catalytic behavior of the catalysts prepared was studied for the SCR of NO by NH_3 in the presence of excess O_2 in the temperature range 250−450 °C. The catalytic tests were performed in a fixed-bed microreactor. The reaction mixture (800 ppm NH_3, 800 ppm NO, and 4% O_2 with nitrogen as balance) was produced by mixing nitrogen (Air Liquide, 99.999%) with NO/N_2 and NH_3/N_2 gaseous mixtures (8861 ppm NO/N_2, 1.02% NH_3/N_2 certified by ±1% and ±5%, respectively, Air Liquide). The concentrations of NO, NO_2, N_2O, NH_3, H_2O, and O_2 in the inlet and outlet of the reactor were quantitatively analyzed using a computer-controlled on-line quadrupole mass spectrometer (VG-Sensorlab 200D).

A 3 mg sample (particle size in the range 100−150 μm) of a catalyst mixed with 97 mg of SiO_2 (Silica gel 60, Merck) was used in these experiments. A mixture of O_2/N_2 containing 10% O_2 was passed through the reactor, and the catalytic bed was heated from room temperature to 100° C where it remained for 45 min. This time was required in order for the signal of 18 amu (H_2O) monitored by the mass spectrometer to be stabilized. The temperature then was increased to 450° C, and the catalyst was heated at this temperature for 45 min. The reaction mixture (flow rate of 150 cm^3 min^{-1} (STP)) was then fed into the reactor, and the molar flow rates, F (mol s^{-1}), of the reactants and products in the inlet (in) and the outlet (out) of the reactor were measured in the temperature range 450−250 °C. Molar flow rate values were then used in order to determine the percentage conversion of NO (x_{NO}, %) for estimating the catalytic activity and the relative percentage yield (Y_{N_2}, %) to the desired product N_2. Expressions 1 and 2 were used, respectively.

$$x_{NO}\,(\%) = \left[\frac{(F_{NO,in} - F_{NO,out})}{F_{NO,in}}\right] \times 100 \qquad (1)$$

$$Y_{N_2}\,(\%) = \left[\frac{(F_{NO,in} + F_{NH_3,in} - F_{NO,out} - F_{NH_3,out} - 2F_{N_2O,out})}{2(F_{NO,in} + F_{NH_3,in})}\right] \times 100 \qquad (2)$$

Catalyst Characterization. *Specific Surface Area (SSA).* Specific surface area measurements have been carried out in a laboratory-constructed apparatus by the three-points dynamic BET method. Pure nitrogen and helium (Air Liquide) were used as adsorption and carrier gas, respectively. The adsorbed amount of nitrogen at a given partial pressure was detected by a thermal conductivity detector of a Varian chromatograph (series 1700).

Fourier Transform Infrared Spectroscopy (FT-IR). Infrared spectra were recorded in a Perkin-Elmer 16 PC FT-IR spectrophotometer, using KBr disks of the prepared catalysts and of the TiO_2 support, in the range 700−1100 cm^{-1}, with a nominal resolution of 2 cm^{-1} and averaging 10 spectra. The anatase spectrum was subtracted from the spectra of the catalysts.

Diffuse Reflectance Spectroscopy (DRS). The diffuse reflectance spectra of the samples studied were recorded in the range 200−800 nm at room temperature (SBW: 2 nm), using a UV−vis spectrophotometer (Varian Cary 3) equipped with an integration sphere. Two series of spectra were recorded. In the first series the PTFE disks of the instrument were used for baseline correction and reference sample. In the second series the TiO_2 carrier was used for the same purposes. The powder samples were mounted in a quartz cell which provided a sample thickness greater than 3 mm.

Laser Raman Microscopy (LRM). The Raman spectra were excited with the 514.5 nm line of a Spectra Physics (Model 163-A42) air-cooled Ar^+ laser. A small-band-pass interference filter was used for the laser plasma lines elimination. The excitation beam was directed to a properly modulated sample compartment of a metallurgical microscope (Olympus BHSM-BH2). The focusing objective lens used for ambient- and high-temperature (345 °C) measurements (via a homemade microfurnace) was either a plano-achromatic 10×/0.30 (MS Plan 10, f = 180) or a long working distance (8 mm) 50×/0.55 Olympus lens. The spectra were obtained with a power of 3 mW on the specimen. The T-64000 (Jobin Yvon) Raman system, equipped with a Spectraview-2DTM liquid N_2-cooled CCD detector, was used in the single spectrograph option. The elastic Rayleigh scattering was removed by a notch holographic filter (HFN-514-1.0 of Kaiser Optical Systems, Inc.). The Raman spectra utilized in the fitting procedure were recorded with a high dispersing element (grating of 1800 grooves/mm^2) at a spectral resolution of 3 cm^{-1}.

X-ray Photoelectron Spectroscopy (XPS). The XPS analysis was performed at room temperature with a SSX-100 model 206 Surface Science Instruments (SSI) photoelectron spectrometer, interfaced to a Hewlett-Packard 9000/310 computer. Experimental details are given elsewhere.[21]

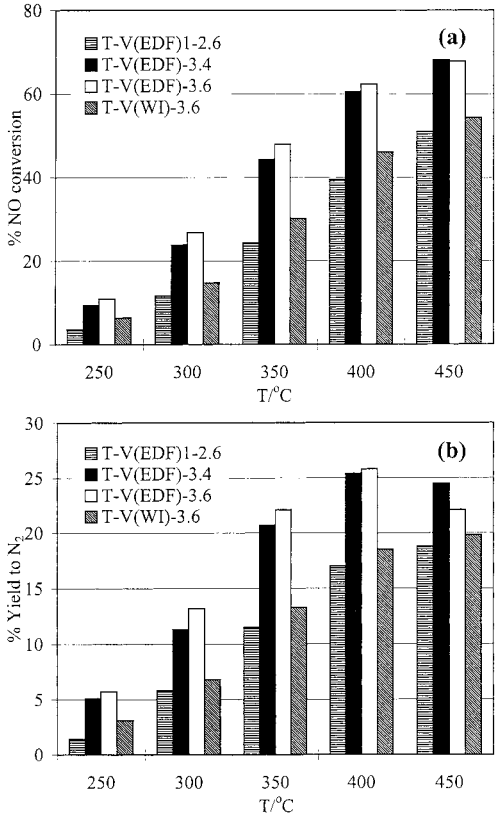

Figure 1. NO conversion (a) and the yield to nitrogen (b) achieved over the EDF catalysts prepared at different pH's and constant concentration of the impregnating solution (1.5×10^{-3} mol $V^{(v)}$ dm^{-3}) and over T-V(WI)-3.6 catalyst.

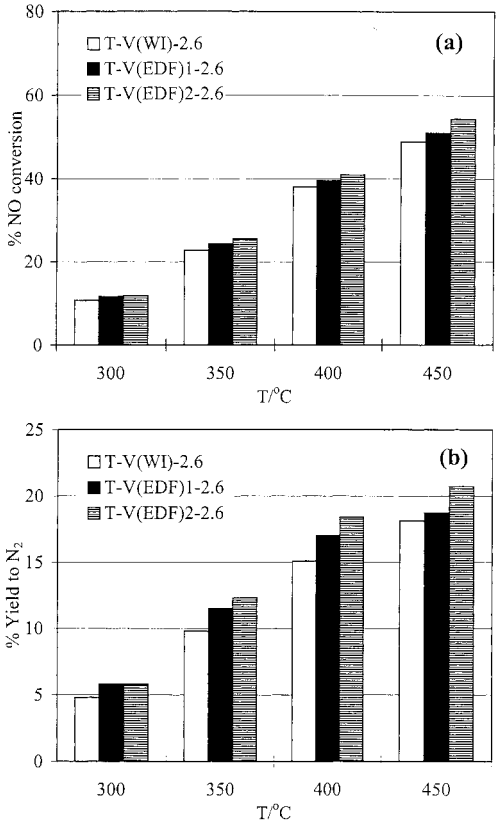

Figure 2. NO conversion (a) and the yield to nitrogen (b) achieved over the EDF and WI catalysts containing 2.6 wt % V_2O_5.

Analytical Electron Microscopy (AEM). Electron microscopy analysis was performed on a JEOL Temscan 100 CX transmitance electron microscope equipped with a Kevex 5100 C energy dispersive spectrometer for X-ray microanalysis. The samples were dispersed in water and deposited on a carbon film supported on a copper grid.

Temperature-Programmed Reduction (TPR). The TPR experiments were performed in a laboratory-constructed equipment described elsewhere[22] in which the ideas of the Rogers−Amenomiya−Robertson arrangement[23] have been followed. A 0.01 g sample was placed in a quartz reactor, and the reducing gas mixture (H_2/Ar: 5/95 v/v) was passed through it for 2 h with a flow rate of 40 cm^3 min^{-1} at room temperature. Then the temperature was increased to 950° C with a constant rate of 10° C min^{-1}. Reduction leads to a decrease of the hydrogen concentration of the gas mixture, which was detected by a thermal conductivity detector (TCD). The reducing gas mixture was dried in a cold trap (−95° C) before reaching the TCD.

Results

Catalytic Activity and Selectivity. Figure 1 illustrates the NO conversion and the relative yield to nitrogen of the EDF catalysts prepared at different pH's and constant concentration of the impregnating solution equal to 1.5×10^{-3} mol $V^{(v)}$ dm^{-3} and of the catalyst with the maximum V loading prepared by wet impregnation. As for the EDF catalysts, it may be observed that in the temperature range 250−450° C the conversion of NO increases with both temperature and the V content. There is only one exception. At the highest temperature studied the T-V(EDF)-3.4 and T-V(EDF)-3.6 samples exhibited almost the same activity. Moreover, it may be observed that the yield of nitrogen increases with both temperature and V content in the temperature range 250−400 °C. Additional increase of temperature brings about a decrease in the relative yield for the samples T-V(EDF)-3.4 and T-V(EDF)-3.6.

From the same figure, it may be seen that the catalyst prepared by EDF (with 3.6 wt % V_2O_5) exhibited both higher conversion of NO and higher yield to nitrogen than the corresponding (i.e., with the same vanadium loading) catalyst prepared by wet impregnation.

Figure 2 illustrates the NO conversion and the relative yield to nitrogen of the EDF catalysts containing 2.6 wt % V_2O_5, prepared under different impregnation conditions, and one catalyst prepared by wet impregnation with the same V loading. As in the previous case it may be seen that the catalysts prepared by EDF exhibited both higher activity and selectivity as compared with the corresponding catalyst prepared by wet impregnation. Moreover, concerning the EDF catalysts it may be seen that the preparation conditions influence both the NO conversion and the yield to nitrogen. The EDF catalyst prepared at pH = 4.5 and initial concentration $C_0 = 6.0 \times 10^{-4}$ mol dm^{-3} (T-V$(EDF)_2$-2.6) is proved to be more active and more selective than the EDF catalyst prepared at pH = 8.0 and $C_0 = 1.5 \times 10^{-3}$ mol dm^{-3} (T-V$(EDF)_1$-2.6) over the whole temperature range studied.

Physicochemical Characterization. *Specific Surface Area (SSA) Measurements.* Table 1 compiles the SSA values of the catalysts studied. It may be observed that the deposition of V species and the calcination followed result, in all cases, to a decrease in the SSA value as compared with the SSA of the support. The magnitude of the effect does not depend on the preparation conditions and the preparation method. This should be partly attributed to the sintering of the supported species taking place in some extent during calcination which in turn close pores of the support with a certain size.[24]

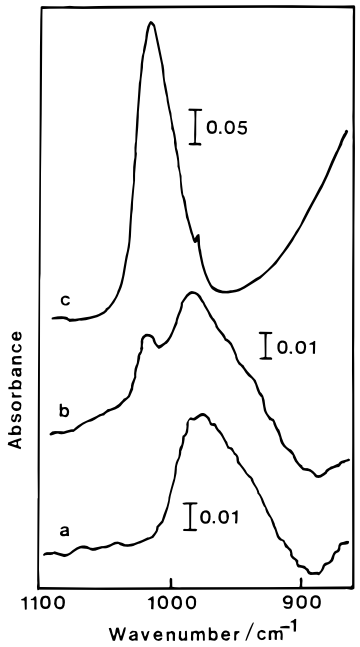

Figure 3. FT-IR spectra of the prepared samples. Spectrum a is representative of all vanadium catalysts prepared besides the T-V(WI)-3.6 sample. Curve b illustrates the spectrum of sample T-V(WI)-3.6 and curve c the spectrum of unsupported V_2O_5.

Fourier Transform Infrared Spectroscopy (FT-IR). Figure 3 illustrates the FT-IR spectra of our samples. Spectrum a is representative of all vanadium catalysts prepared besides the T-V(WI)-3.6 sample. Curve b illustrates the spectrum of sample T-V(WI)-3.6, and curve c the spectrum of unsupported V_2O_5. A large band centered in the region 980−987 cm^{-1} and presenting an asymmetry toward the low wavenumber side is detected in all catalysts studied (curves a and b). This is attributed to the stretching vibrations of the $(V{=}O)^{3+}$ bond of a variety of monolayered $V^{(v)}$ species supported on titania (amorphous VO_x).[7,25−29] The above-mentioned variety is responsible for the observed asymmetry. An additional band centered at about 1022 cm^{-1} is detected in the spectrum of the T-V(WI)-3.6 catalyst (spectrum b). This band is due to the double bond V═O of the V_2O_5 (see spectrum c) and suggests the presence of V_2O_5 supported crystallites in this catalyst.[30] It is worth noting that this band is not observed in the FT-IR spectrum of the T-V (EDF)-3.6 catalyst.

In conclusion, the FT-IR spectra of the prepared catalysts showed the presence of well-dispersed vanadium species (presumably monolayered species). The formation of V_2O_5 supported crystallites was only observed in the T-V(WI)-3.6 sample.

Analytical Electron Microscopy (AEM). Figure 4a illustrates the electron microscopy photograph of the T-V(EDF)-3.6 catalyst. It may be seen that the catalyst particles seem to be rather homogeneous. Particles containing V_2O_5 crystallites were not detected. The same picture is observed in all catalysts prepared by EDF.

Figure 4b illustrates a representative electron microscopy photograph of the T-V(WI)-3.6 catalyst prepared following wet impregnation. The heterogeneity of this sample is obvious. More precisely, region 3 is very similar to the appearance of the EDF samples, while regions 1 and 2 are different in appearance and, as shown by microanalysis, consist mainly of vanadia phase in which titania particles are incorporated. Well-formed crystallites of V_2O_5 were also detected in this sample.

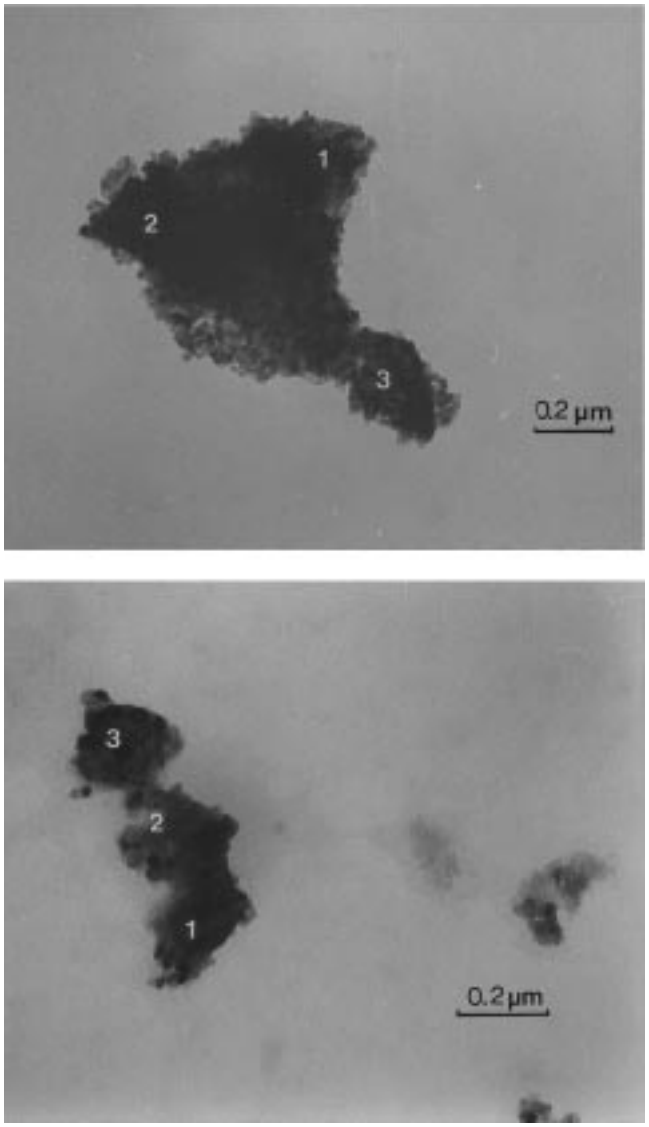

Figure 4. Representative electron microscopy photographs of the T-V(EDF)-3.6 (a) and Ti-V(WI)-3.6 (b) catalysts. As shown by microanalysis a1, a2, and a3 have the same composition consisting of both vanadium and titanium. This is also the case for region b3. In contrast, regions b1 and b2 consist mainly of vanadium phase in which some titania particles are incorporated.

Figure 5 illustrates histograms of microanalysis of the catalysts T-V (EDF)-3.6 (a), T-V(EDF)-3.4 (b), and T-V(WI)-3.6 (c). The atomic ratio V/Ti, determined at various particles of the aforementioned catalysts, shows that the EDF catalysts exhibit more homogeneous distribution of the supported vanadium than the WI catalyst. The same picture is observed for the catalysts containing 2.6 wt % V_2O_5. The above are in full agreement with the electronic microscopy photographs presented before.

Diffuse Reflectance Spectroscopy (DRS). Figures 6 and 7 illustrate the diffuse reflectance spectra respectively of the prepared catalysts and those of a $V_2O_5{-}TiO_2$ mechanical mixture submitted in various treatments. All these spectra were recorded using TiO_2 as a reference. An intense band in the range 350−550 nm with a maximum centered at about 415 nm has been observed in all cases.

According to the literature,[26,27,31−33] $V^{(v)}$ species in octahedral symmetry gives a band in the range 400−480 nm which is attributed to the charge-transfer processes of $V^{(v)}$ ions in the decavanadate species. When the coordination of the $V^{(v)}$ is

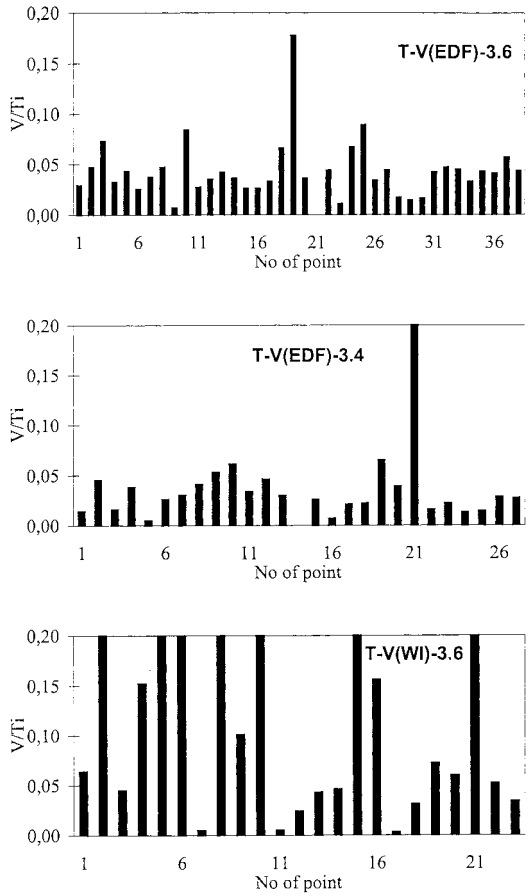

Figure 5. Histograms illustrating the variation of the V/Ti atomic ratios measured by X-ray microanalysis in various particles of the catalysts T-V(EDF)-3.6, T-V(EDF)-3.4, and T-V(WI)-3.6.

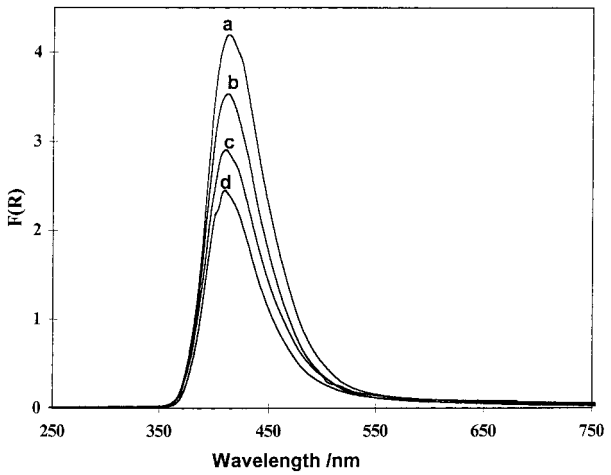

Figure 6. Diffuse reflectance spectra of the catalysts T-V(EDF)-3.6 (a), T-V(EDF)-3.4 (b) T-V(WI)-3.6 (c), T-V(EDF)$_1$-2.6 (d), T-V(EDF)$_2$-2.6 (d), and T-V(WI)-2.6 (d) recorded using TiO_2 as a reference.

tetrahedral, this band is observed in wavelengths below 350 nm. The crystalline V_2O_5 gives a band in the region 500−540 nm attributed to the charge-transfer processes $O^{2-} \rightarrow V^{5+}$. Finally, $V^{(iv)}$ gives a DR band in the range 550−700 nm which is attributed to the d−d transitions of the octahedral VO^{2+} species. According to several authors,[34,35] an intense band centered at about 410−415 nm appears in the DR spectra of TiO_2 when it is doped with transition elements. This is attributed to the charge-transfer process $M^{n+} \rightarrow Ti^{4+}$. In the case of $V^{(v)}$ there are not d electrons to be given to TiO_2. The presence, therefore,

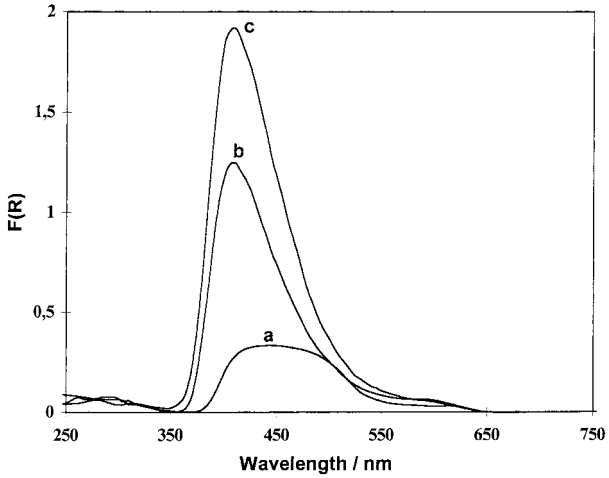

Figure 7. Diffuse reflectance spectra of a $V_2O_5-TiO_2$ mechanical mixture containing 3.6 wt % of V_2O_5 after simple mixing (a), after mixing, soaking, and drying (b), and after mixing, soaking, drying, and calcination (c).

of the intense band at 410−415 nm in the case of the V_2O_5/TiO_2 catalysts has been attributed to the formation of oxygen-containing vanadate species of octahedral symmetry on the support surface.[35]

To further investigate this point, we recorded the DR spectra of a $V_2O_5-TiO_2$ mechanical mixture containing 3.6 wt % V_2O_5 after various treatments. This mixture has been prepared by simultaneous grinding of the two components in an achate mortar. The recorded spectra are illustrated in Figure 7. As can be seen, the spectrum of the initially prepared mechanical mixture (curve a) exhibits a weak shoulder in the region 380−550 nm. This shoulder has been transformed into a peak centered at ∼415 nm in the spectrum (curve b) recorded after wetting and drying overnight at 120° C the above mixture. Finally, the intensity of this band has been further increased in the spectrum (curve c) recorded after calcination for 5 h at 500° C of the previously wetted and dried mechanical mixture. The above consequence of treatments is expected to increase gradually the interactions between the vanadia phase and the TiO_2. As was already mentioned, this increase was reflected by an increase in the DR band centered at ∼415 nm.

Let us turn back to Figure 6. It may be observed that in the case of the catalysts prepared by EDF the intensity of the above-mentioned peak (spectra a, b, and d) increases with the vanadium content, suggesting that the amount of the interaction species also increase with the V content. It should be noticed that the catalysts T-V(EDF)$_1$-2.6 and T-V(EDF)$_2$-2.6 provided identical spectra (curve d).

Concerning the DR spectra of the catalysts T-V(EDF)-3.6 and T-V(WI)-3.6, it may be seen that the intensity of the peak at 415 nm is significantly higher for the EDF catalyst than the corresponding one of the WI catalyst with the same vanadium content. It seems that "vanadia phase−titania" interactions are maximized in the EDF preparation. This is also evident from the DR spectra taken using PTFE as a reference (Figure 1S). This is not the case for the T-V(EDF)$_{1 \text{ or } 2}$-2.6 and T-V(WI)-2.6 which provided identical DR spectra. However, from the DR spectra of the catalysts containing 2.6 wt % V_2O_5 recorded using PTFE as a reference (so that information can also be obtained from the region of 200−350 nm), one can conclude that the coverage of the support was higher in the case of the EDF-prepared catalysts and also that the maximum coverage is achieved in the T-V(EDF)$_1$-2.6 sample which was prepared by EDF at pH = 8 (Figure 2S).

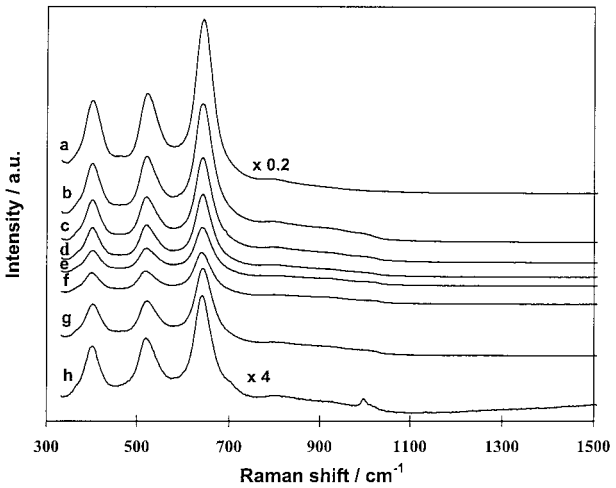

Figure 8. Raman spectra of the anatase (a) and the prepared catalysts: T-V(WI)-2.6 (b), T-V(EDF)$_2$-2.6 (c), T-V(EDF)$_1$-2.6 (d), T-V(EDF)-3.4 (e), T-V(EDF)-3.6 (f), and T-V(WI)-3.6 (g and h, depending on the point where the laser beam was focused).

Laser Raman Microscopy (LRM). The Raman spectra of the support and the prepared catalysts (Figure 8) exhibited the characteristic peaks of anatase at 400, 520, 643, and 794 cm^{-1}.[36−39] The coverage of the support surface by the vanadia phase provoked a considerable decrease in the intensity of the above peaks. This effect increases with the V loading, and for the same composition, it is higher in the EDF-prepared samples. This strongly suggests that the EDF results to V_2O_5/TiO_2 catalysts with relatively higher dispersion of the vanadia phase. As for the two catalysts prepared by EDF which contain the same amount of vanadia phase (2.6 wt % V_2O_5), it may be seen that higher dispersion is achieved in the sample prepared at pH = 8.0 in full agreement with the DRS results (see Figure 2S).

Every sample studied provided identical spectra irrespective of the point of the sample where the incident laser beam was focused; the only exception was the T-V(WI)-3.6 catalyst, for which a peak at 997 cm^{-1} was observed for several illumination points (Figure 8, curves g and h). The presence of this peak, which is attributed to the symmetrical stretching vibrations of the extreme oxygen atoms, υ(V═O) of the crystalline V_2O_5, strongly suggests lower dispersion of the supported vanadium phase and confirms the formation of V_2O_5 crystallites in this catalyst in agreement with the AEM and FT-IR results.

In the following we shall study the broad band observed in the range 750−1050 cm^{-1}, under ambient and dehydrated conditions, for all catalysts prepared. This band was analyzed into Gaussian type peaks as can be seen in Figure 9. In all cases the best fitting has been achieved by deconvoluting the aforementioned broad band into five peaks. For all samples (Raman spectra taken under either ambient or dehydrated conditions) the first peak centered at 800 ± 5 cm^{-1} appeared in the spectra of all catalysts studied as well as in the spectrum of anatase. Therefore, in accordance with the literature[40] it may be attributed to the latter. As the anatase does not provide Raman peaks at higher wavenumbers, the remainder of the peaks are attributed to the supported V species.[41] These are centered in the ranges 826−838, 922−930, and 990−995 cm^{-1} and at 1012 cm^{-1} for the hydrated samples and at 841−865, 915−932, 1012−1018, and 1026−1031 cm^{-1} for the dehydrated ones.

According to the literature, a peak at 820−860 cm^{-1} is attributed to the stretching vibrations of the υ(V−O−V) bond of the polymeric octahedral decavanadate species.[29,42,43] This peak appeared in the Raman spectrum of the $Na_6V_{10}O_{18}\cdot 18H_2O$ where decavanadate ions are present,[44] as well as the solids $K_2Zn_2V_{10}O_{28}\cdot 16H_2O$, $Ca_3V_{10}O_{28}\cdot 15H_2O$, and $K_2Mg_2V_{10}O_{28}\cdot 16H_2O$ which also contain the $(V_{10}O_{28})^{6-}$ ions. A peak at 920−930 cm^{-1} is attributed to the stretching vibration of the bond υ(V═O) of the polymeric tetrahedral metavanadate ions.[42,44−47] Specifically, according to Baiker et al.,[48] the chains of the metavanadate species provide a band at 945 cm^{-1}. Upon condensation of these chains into ribbons, the frequency decreased to 920 cm^{-1}. A peak at 980−1000 cm^{-1} is due to the stretching vibrations of the υ(V═O) bond of the species, mentioned previously, which are responsible for the peak at 826−838 cm^{-1}.[42,44,49] A sharp peak that suggests the presence of crystalline V_2O_5 (997 cm^{-1}) also appears in the same region. A peak at 1010−1020 cm^{-1} is attributed to the stretching vibrations of the υ(V═O) bond in the monomeric or oligomeric vanadyl species.[3,42,45,48] According to Baiker et al.,[48] the structure of vanadium in these species is similar to that described above for the vanadate ribbons. The tetrahedral symmetry in this case is also supported by the work reported by Handy et al.[45] Finally, a peak at 1020−1030 cm^{-1} has been attributed to a surface tetrahedral structure possessing one short apical V═O bond and three intermediate bridging bonds.[6]

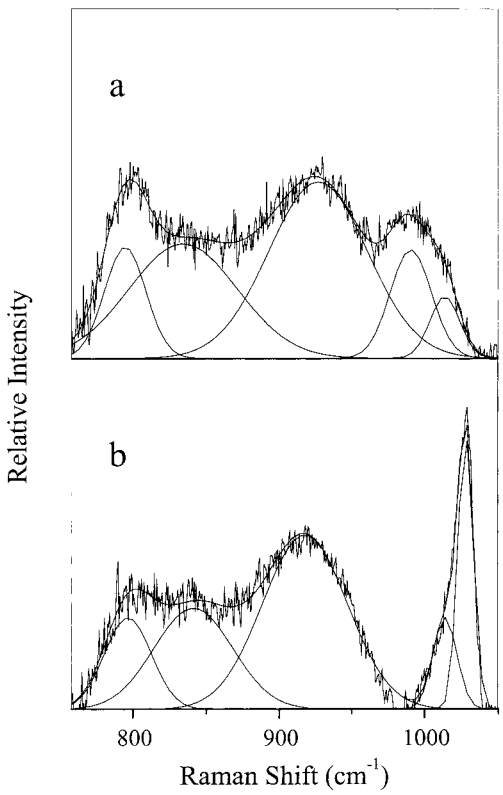

Figure 9. Typical Raman spectra in the range 750−1050 cm^{-1} recorded under ambient (a) and dehydrated (b) conditions. Deconvolution of the Raman bands was performed by applying a linear baseline correction and a fixed area for the second-order peak of anatase at ca. 800 cm^{-1}. The fixed area was calculated taking into account the areas ratio of the above peak over the anatase peak at ca. 640 cm^{-1} (not appearing in this figure) for the titania support and the area of the later peak for each sample.

Comparing the Raman spectra taken under ambient conditions with the corresponding ones taken under dehydrated conditions (Figure 9), the main difference observed is the disappearance of the peak centered at 990−995 cm^{-1} and the simultaneous appearance of the peak at 1026−1031 cm^{-1} for the dehydrated samples. This phenomenon has been interpreted as due to the change in the coordination of the surface vanadia species from

TABLE 2: Atomic Ratios $(V/Ti)_{bulk}$, $(V/Ti)_{XPS}$, $(V^{(v)}/Ti)_{XPS}$, $(V^{(iv)}/Ti)_{XPS}$, and $(V^{(iv)}/V_{total})_{XPS}$ for the Catalysts Studied

sample	$(V/Ti)_{bulk}$ ($\times 10^3$)	$(V/Ti)_{XPS}$ ($\times 10^3$)	$(V^{(v)}/Ti)_{XPS}$ ($\times 10^3$)	$(V^{(iv)}/Ti)_{XPS}$ ($\times 10^3$)	$(V^{(iv)}/V_{total})_{XPS}$
T-V(EDF)$_1$-2.6	23.45	127.6	45.9	81.6	0.64
T-V(EDF)$_2$-2.6	23.45	126.8	19.5	104.9	0.82
T-V(WI)-2.6	23.45	122.3	45.9	74.3	0.61
T-V(EDF)-3.4	30.90	157.6	56.8	98.2	0.62
T-V(EDF)-3.6	32.80	168.0	63.5	99.7	0.59
T-V(WI)-3.6	32.80	154.8	68.8	88.5	0.57

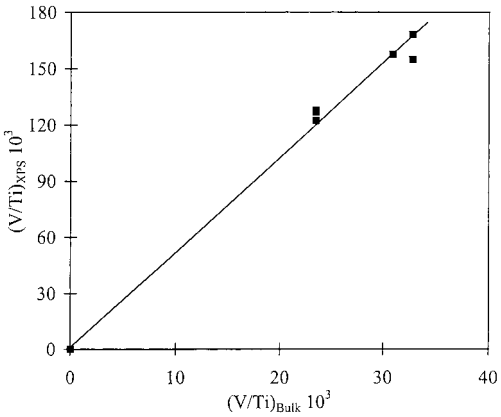

Figure 10. Dependence of the V/Ti atomic ratio determined by XPS on the corresponding bulk ratio of the catalysts studied.

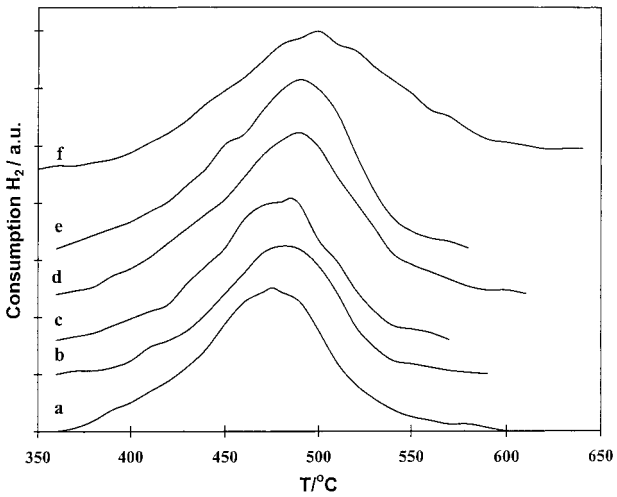

Figure 11. TPR curves of the catalysts T-V(EDF)$_1$-2.6 (a), T-V(EDF)-3.4 (b), T-V(EDF)$_2$-2.6 (c), T-V(WI)-2.6 (d), T-V(EDF)-3.6 (e), and T-V(WI)-3.6 (f).

octahedral to tetrahedral upon dehydration, as revealed by solid-state ^{51}V NMR.[50]

The relative intensities of the observed peaks under either ambient or dehydrated conditions are not influenced by both the V content (in the range used here) and the preparation conditions.

X-ray Photoelectron Spectroscopy (XPS). From the XP spectra of the catalysts studied we calculated the values of the binding energies of the Ti $2p_{3/2}$ and V $2p_{3/2}$ photoelectrons. The first value was found to be equal to 458 ± 0.1 eV, which is characteristic of TiO_2. The value of the latter was found to be equal to 516.3 ± 0.1 eV. This value falls between the values 517.1 and 516 eV, which are characteristic of the V $2p_{3/2}$ photoelectrons of the $V^{(v)}$ and $V^{(iv)}$ ions, respectively.[51,52] According to the literature,[53] this shift of the XPS peak corresponding to V $2p_{3/2}$ photoelectrons to lower values than 517.1 eV indicates the presence of the $V^{(iv)}$ ions. Indeed, the deconvolution of the peak appearing at 516.3 eV into two peaks centered at 517.0 ± 0.1 and 516.0 ± 0.2 eV provided the best fitting in our XPS spectra, showing the presence of $V^{(iv)}$ ions, in addition to the $V^{(v)}$ ions, in our samples.

The aforementioned deconvolution allowed us to calculate the surface atomic ratios $(V^{(v)}/Ti)_{XPS}$ and $(V^{(iv)}/Ti)_{XPS}$ in addition to the surface atomic ratio $(V/Ti)_{XPS}$. The values of these ratios are compiled in Table 2 together with the values of the bulk atomic ratio $(V/Ti)_{bulk}$. It may be seen that the ratio $(V/Ti)_{XPS}$ increased with the vanadium content, which is rather predictable as the amount of the supported vanadium in our samples is smaller than that corresponding to the monolayer.[54] This increase is quite linear as may be seen in Figure 10. An inspection of Table 2 clearly shows that the values of $(V/Ti)_{XPS}$ are higher in the EDF than in the corresponding WI catalysts. This suggests that EDF results to relatively high dispersity of the supported vanadia phase. As for the catalysts with vanadium content equal to 2.6 wt % V_2O_5 prepared by EDF, it may be observed that the catalyst prepared at pH = 8 exhibits higher $(V/Ti)_{XPS}$ value and, therefore, higher dispersity of the vanadia phase in agreement with the DRS (Figure 2S) and LRM (Figure 8) results. Inspection of Table 2 also shows that the valence of a large portion of the surface vanadium is equal to four in agreement with the literature.[30]

Temperature-Programmed Reduction (TPR). Figure 11 illustrates the TPR curves of the catalysts studied. An intense peak, centered at about 480° C, may be observed in all cases. According to the literature,[55,56] this peak is attributed to the reduction $V^{(v)} \Rightarrow V^{(iii)}$ of the surface polyvanadate species.[57] The TPR curve of the T-V(WI)-3.6 catalyst exhibits, in addition, remarkable reduction even at temperatures higher than 650° C. In fact, only in this case does the TPR curve not return to the baseline under our experimental conditions. This phenomenon, observed in the catalyst with relatively high V content,[57,58] reflects, presumably, the presence of V_2O_5 crystallites on the titania surface. In view of the AEM, FT-IR, and LRM results mentioned above, this is indeed the case in our system.

Inspection of Figure 11 shows that the EDF catalysts are reduced easier (at lower temperatures) than the corresponding catalysts prepared by wet impregnation. Taking into account that the increase of the vanadium supported phase−titania interactions increases the reducibility,[58,59] one may infer that these interactions are stronger in the EDF catalysts, which in turn suggests better dispersion in agreement with DRS, LRM, XPS, and AEM results mentioned in previous sections. Inspection, moreover, of Figure 11 shows that the T-V(EDF)$_1$-2.6 catalyst is reduced easier than the T-V(EDF)$_2$-2.6 catalyst, suggesting stronger supported phase−support interactions and presumably better dispersity of the supported phase in the first sample in agreement with the DRS and LRM results mentioned in previous sections. Finally, it may be observed that increase of the vanadium content in the EDF catalysts increases the reduction temperature, suggesting decrease of the vanadium phase−titania interactions.

Temperature-Programmed Desorption of Ammonia (TPD). Figure 12 illustrates the TPD NH_3 diagrams of the prepared catalysts as well as of the titania used as support. On the TPD

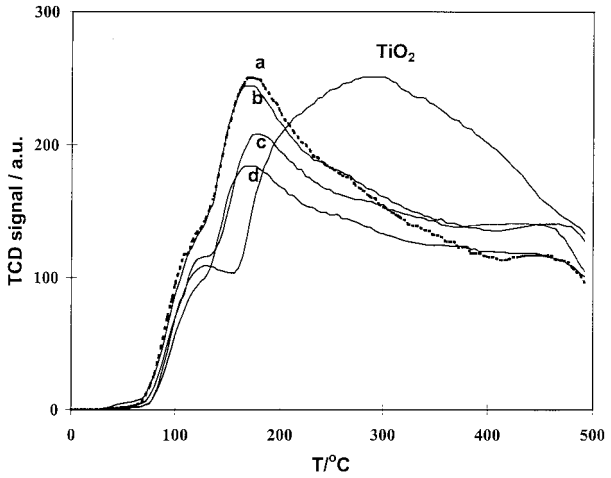

Figure 12. TPD of NH_3 curves of the catalysts prepared: (a) T-V(EDF)-3.6, (b) T-V(EDF)-3.4, (c) T-V(EDF)$_{1 \text{ or } 2}$-2.6 and T-V(WI)-2.6, and (d) T-V(WI)-3.6.

NH_3 diagram of anatase a quite sharp peak is centered at about 100−120° C along with a broad signal with maximum at about 300° C. The first peak is attributed to the desorption of the physisorbed ammonia[53] while the second to the Lewis acid sites (LAS) of anatase.[60,61] The formation of vanadia supported phase is responsible for the appearance of an additional signal at about 170−180° C. This signal may be attributed to the Brönsted acid sites (BAS) exclusively located on the vanadia supported phase.[53] It may be seen that in the case of the catalysts prepared by EDF the intensity of this signal increases with the vanadium content, which is in agreement with the literature.[53,60,62] The corresponding decrease observed in the intensity of the broad signal centered at about 300° C may be attributed to the coverage of the titania LAS by the supported vanadia phase.

Comparing the TPD NH_3 curves of the catalysts with the maximum vanadium content prepared by EDF and wet impregnation, it may be seen that the magnitude of the peak due to the BAS is larger in the EDF than in the WI sample.

Discussion

Influence of the Preparation Method on the Physicochemical and Catalytic Properties of the V_2O_5/TiO_2 Catalysts. To investigate whether the details of the preparation method followed influence the physicochemical characteristics and thus the catalytic behavior of the vanadia supported titania catalysts was the first goal of the present study.

The appearance of a band in the 980−987 cm^{-1} region of the FT-IR spectra of the catalysts studied (Figure 3) indicated the formation of the monolayered amorphous phase of the supported $V^{(v)}$ species in all specimens studied irrespective of the preparation method followed. However, there are remarkable differences between the EDF and the corresponding WI catalysts.

The most important difference is the formation of the V_2O_5 crystallites on the titania surface in the WI catalyst with the maximum V content. The appearance of a FT-IR band at 1022 cm^{-1} (Figure 3), the remarkable reduction showed by the TPR diagram even at temperatures higher than 650° C (Figure 11, curve f), and the appearance of a sharp band at 997 cm^{-1} in the LRM spectrum (Figure 8) strongly suggest the formation of this phase in the V-T(WI)-3.6 catalyst. Additional evidence for the formation of this phase provides the AEM micrographs (Figure 4c) and the histogram illustrating the V/Ti atomic ratios measured in various particles of this catalyst (Figure 5c).

Taking into account that even in the catalyst T-V(WI)-3.6 the concentration of the supported phase is lower than that corresponding to the theoretical monolayer (0.1 wt % V_2O_5 per m^2 of the support), the formation of the supported crystallites should be attributed to the relatively bad dispersion of vanadia phase due to the preparation method used, namely wet impregnation.[37,63]

Also, another important difference between the catalysts prepared by EDF and the corresponding ones prepared by WI is the difference in the homogeneity of the distribution of the vanadia phase on the support particles. In fact, the AEM micrographs and the corresponding microanalysis results (Figures 4 and 5) showed that in the EDF catalysts the vanadia phase is distributed more uniformly on the titania particles as compared with the WI catalysts.

The surface coverage of the support by the vanadia phase is also influenced by the preparation method. A first evidence for the relatively bad dispersion of the vanadia phase in the catalysts prepared by WI is the formation of the V_2O_5 crystallites in the T-V(WI)-3.6 catalyst mentioned before. Moreover, the lower intensities of the LR peaks of the support (Figure 8) and the lower values of the $F(R)$ function in the range 200−400 nm (Figures 1S and 2S) in the EDF than in the WI catalysts as well as the XPS results (Table 2) and the fact that the TPD of NH_3 diagrams show that the size of the peak due to the BAS, mainly located on the vanadia phase, is larger in the T-V(EDF)-3.6 than in the T-V(WI)-3.6 catalyst strongly suggest that EDF results in V_2O_5/TiO_2 catalysts with a high dispersity of the vanadia phase and thus to catalysts with a high surface coverage of the titania surface by the vanadia supported phase.

The supported vanadia−titania interactions are also influenced by the preparation method. It is generally accepted that the forementioned interactions are quite strong in the V_2O_5/TiO_2 catalysts, and this renders titania the best support for the preparation of these catalysts.[31,41,64] The nature of these interactions is not fully elucidated though some authors reported that these are due to the structural similarity of the V_2O_5 and anatase.[31] The extent and the strength of these interactions are investigated in the present study by the joint use of DRS, XPS, and TPR.

The appearance of an absorption band in DR spectra, recorded using TiO_2 as a reference sample (Figure 6), with a maximum centered at ∼415 nm has been attributed to the formation of oxygen-containing species of octahedral symmetry on the titania surface.[34] According to Malet et al.,[35] these species are of the hyperoxy structure (V−O−O−V) and are stabilized on the titania surface as a result of the interactions developed between the supported vanadia phase and the structure of anatase. Our results confirmed that the size of the peak observed at ∼415 nm can be taken as a measure of the extent of these interactions. Comparison of spectra a and c of Figure 6 clearly shows that EDF results in the supported catalysts with greater amount of "vanadia phase−anatase" interaction species as is compared with the conventional wet impregnation.

The presence of $V^{(iv)}$ species on the surface of titania, observed by various investigators in the past,[28,30,51,52] has been attributed to various reasons as contradictory results have been reported. However, regardless of the exact mechanism via which the formation of $V^{(iv)}$ species takes place on the TiO_2 surface, it seems well established that these species are formed through the interaction of vanadium with specific sites of the TiO_2 surface in aerobic conditions and without the presence of a reducing reagent. So, the presence of these species indicates the development of quite strong interactions between the vanadia

phase and the anatase surface. Therefore, the ratio $(V^{(iv)}/V_{total})_{XPS}$ can be taken as a measure of these interactions. Inspection of Table 2 shows that this ratio is greater in the EDF than in the corresponding WI catalysts, suggesting again extended "vanadia phase−anatase" interactions.

Taking into account our TPR results, we can conclude that the strength of the above interactions is also influenced by the preparation method. More precisely, the observation that the reduction of the EDF catalysts takes place at lower temperatures than those for the corresponding WI catalysts (Figure 11) strongly suggests that stronger interactions are developed in the first case. However, these interactions seem to be weakened as the vanadium content increases.

Besides the formation of crystalline V_2O_5 on the T-V(WI)-3.6 sample, no other influence of the preparation method on the structure of the V supported species could be detected by LRM. However, recording of LRM spectra of our samples (Figure 9) under various hydration conditions confirmed previous findings,[6] namely, the important influence of the hydration degree on the relative concentrations and the nature of surface V species. Consequently, the evaluation of the intrinsic activity of the various V species should be based on LRM spectra recorded in situ.

We should note here that the influence of the preparation method on both the physicochemical and catalytic properties is significantly more evident in the samples containing the higher V loading (3.6 wt % V_2O_5). For these samples, the application of EDF results in V_2O_5/TiO_2 catalysts with relatively high dispersity of active phase, homogeneous distribution of the vanadia phase on the support particles, and extended and stronger interactions between the vanadia supported phase and the surface of titania. Moreover, EDF inhibits the formation of V_2O_5 crystallites. In view of the above one may understand why EDF catalysts exhibited better activity and selectivity than the conventional WI catalysts (see Figures 1 and 2). For the samples with the lower V content the influence of the preparation method is less pronounced.

Influence of the Impregnation Parameters on the Physicochemical and Catalytic Properties of the V_2O_5/TiO_2 Catalysts with the Same V Content Prepared by EDF. To investigate whether the change in the impregnation parameters may be used to regulate the physicochemical and catalytic properties of the EDF V_2O_5/TiO_2 catalysts, we prepared two samples, T-V$(EDF)_1$-2.6 and T-V$(EDF)_2$-2.6, with the same V content but using different impregnation parameters (see Table 1).

The lower intensities of the LR peaks of the support (Figure 8), the lower values of the $F(R)$ function in the range 200−400 nm (Figure 2S), and the higher value for the $(V/Ti)_{XPS}$ ratio exhibited by the T-V$(EDF)_1$-2.6 sample as compared with the corresponding values exhibited by the T-V$(EDF)_2$-2.6 sample (Table 2) show that the increase in the pH of the impregnating solution causes a slight increase in the dispersity of the active phase and thus in the surface coverage of titania by the vanadia phase. On the other hand, on the basis of the DRS, XPS, and TPR results, it is not easy to see whether the increase in the impregnation pH influences the "vanadia phase−titania" interactions. Finally, our TPD of NH_3 results (Figure 12, curve c) showed that the change of the impregnation parameters (namely of the initial concentration and the impregnation pH in the corresponding ranges of 6.0×10^{-4} to 1.5×10^{-3} mol dm^{-3} and 4.5 to 8.0) while keeping the loading constant (2.6 wt % V_2O_5) did not have any detectable influence on the acidic characteristics of these catalysts.

Moreover, taking into account the minor differences in the catalytic performance of these two samples, we may conclude that the change of the impregnation parameters (in the range of values used) does not influence in any significant way the physicochemical and catalytic properties.

Influence of the Impregnation pH on the Physicochemical and Catalytic Properties of the V_2O_5/TiO_2 Catalysts Prepared by EDF. The most important consequence of the decrease of the impregnation pH in the EDF preparations (while keeping constant the concentration of impregnating solution) is the increase of the amount of the vanadium species deposited on the titania surface. In a recent study our group has fully elucidated the mechanism of this deposition and explained this effect.[11] The increase in the amount of the deposited vanadia species causes, in turn, very important changes in the physicochemical characteristics of the EDF catalysts. To be specific, the magnitude of the surface coverage increased with the vanadium content. This is manifested by the decrease in the intensity of the LR bands of the support (Figure 8), the increase of the $(V/Ti)_{XPS}$ ratio (Figure 10 and Table 2), and the increase of the peak due to the BAS, mainly located on the vanadia phase (Figure 12). On the other hand, the increase, with the vanadia content, in the intensity of the DRS band (Figure 6) and the increase in the ratio $(V^{(iv)}/Ti)_{XPS}$ (Table 2) indicate an increase in the amount of the vanadium species strongly interacting with the titania surface. However, the relative amount of these species and, therefore, the mean value of the vanadia supported phase−support interactions decreased with vanadium content as is manifested by the progressive decrease in the ratio $(V^{(iv)}/V_{total})_{XPS}$ (Table 2) and the increase of the temperature corresponding to the maximum of the TPR large peak (Figure 11). The latter effect has been reported by Bond et al.[58] Finally, the increase of the V content is accompanied by an increase in both activity and selectivity (Figure 1).

Conclusions

The most important findings of the present study are the following:

I. The application of EDF results in V_2O_5/TiO_2 catalysts with relatively high dispersity of the vanadia supported phase, homogeneous distribution of this phase on the support particles, quite extended and strong interactions between the supported vanadia phase and the support surface, and inhibition of the formation of the supported V_2O_5 crystallites. The above explain the relatively high activity and selectivity of the V_2O_5/TiO_2 catalysts prepared by EDF as compared to the corresponding catalysts prepared by the conventional wet impregnation.

II. Decrease of the impregnation pH in the EDF preparations causes an increase of the V content, an increase of the surface coverage of the titania surface by the vanadia phase, and a decrease of the mean value of the vanadia phase−support interactions. The above explained the increase in activity and selectivity of the V_2O_5/TiO_2 catalysts with the V content.

III. The change of the impregnation parameters (pH and concentration of impregnation solution) does not influence significantly the physicochemical and catalytic properties of the V_2O_5/TiO_2 catalysts prepared by EDF when the V loading is kept constant.

Acknowledgment. Financial support by the European Union (Project ENVIRONMENT, Contract No. EV5V-CT92-0234) is gratefully acknowledged. Financial support to I. Georgiadou from the Greek Award Granting Authority (IKY) is also gratefully acknowledged.

Supporting Information Available: Description of two figures (1S, 2S) illustrating DR spectra of the catalysts recorded using PTFE as reference (3 pages). See any current masthead page for ordering information and Web access instructions.

References and Notes

(1) Topsoe, N.-Y.; Dumesic, J. A.; Topsfe, H. *J. Catal*. **1995**, *151*, 241.
(2) Topsoe, N.-Y. *Science* **1994**, *265*, 1217.
(3) Lietti, L.; Forzatti, P. *J. Catal.* **1994**, *147*, 241.
(4) Topsoe, N.-Y.; Topsfe, H.; Dumesic, J. A. *J. Catal.* **1995**, *151*, 226.
(5) Ciambelli, P.; Lisi, L.; Russo, G.; Volta, J. C. *Appl. Catal*. **1995**, *7*, 1.
(6) Machej, T.; Haber, J.; Turek, A. M.; Wachs, I. E. *Appl. Catal*. **1991**, *70*, 115.
(7) Roozeboom, E.; Mittelmeijer-Hazeleger, M. C.; Moulijn, J. A.; Medema, J.; de Beer, V. H. J.; Gellings, P. J. *J. Phys. Chem*. **1980**, *84*, 2783.
(8) Kantcheva, M.; Davydov, A.; Hadjivanov, K. *J. Mol. Catal*. **1993**, *81*, L25.
(9) Kantcheva, M.; Bushev, V.; Klissurski, D. *J. Catal*. **1994**, *145*, 96.
(10) Kantcheva, M. M.; Hadjivanov, K. I.; Klissurski, D. *J. Catal*. **1992**, *134*, 299.
(11) Bourikas, K.; Georgiadou, I.; Kordulis, Ch.; Lycourghiotis, A. *J. Phys. Chem. B* **1997**, *101*, 8499.
(12) Spanos, N.; Slavov, S.; Kordulis, Ch.; Lycourghiotis, A. *Langmuir* **1994**, *10*, 3134.
(13) Spanos, N.; Lycourghiotis, A. *Langmuir* **1994**, *10*, 2351.
(14) Karakonstantis, L.; Bourikas, K.; Lycourghiotis, A. *J. Catal*. **1996**, *162*, 295.
(15) Spanos, N.; Slavov, S.; Kordulis, Ch.; Lycourghiotis, A. *Colloids Surf*. **1995**, *97*, 109.
(16) Bourikas, K.; Spanos, N.; Lycourghiotis, A. *Langmuir* **1997**, *13*, 435.
(17) Spanos, N.; Lycourghiotis, A. *J. Catal*. **1994**, *147*, 57.
(18) Bourikas, K.; Spanos, N.; Lycourghiotis, A. *J. Colloid Interface Sci*. **1996**, *184*, 301.
(19) Georgiadou, I.; Spanos, N.; Papadopoulou, Ch.; Matralis, H.; Kordulis, Ch.; Lycourghiotis, A. *Colloids Surf.* **1995**, *98*, 155.
(20) Snell, F. D. In *Photometric and Fluorometric Methods of Analysis of Metals*; Wiley: New York, 1978; Vol. 2, p 1235.
(21) Fountzoula, Ch.; Matralis, H. K.; Papadopoulou, Ch.; Voyatzis, G. A.; Kordulis, Ch. *J. Catal.* **1997**, *172*, 391.
(22) Spanos, N.; Matralis, H. K.; Kordulis, Ch.; Lycourghiotis, A. *J. Catal*. **1992**, *136*, 432.
(23) Lemaitre, J. L. In *Characterization of Heterogeneous Catalysts;* Delanay, F., Ed.; Dekker: New York, 1984; Chapter 1.
(24) Saleh, R. Y.; Wachs, I. E.; Chan, S. S.; Chersich, C. C. *J. Catal.* **1986**, *98*, 102.
(25) Centi, G.; Pinelli, D.; Trifiro, F.; Ghoussoub, D.; Guelton, M.; Gengembre, L. *J. Catal.* **1991**, *130*, 238.
(26) Kantcheva, M. M.; Hadjiivanon, K. I.; Klissurski, D. G. *J. Catal*. **1992**, *134*, 299.
(27) Andersson, A. *J. Catal.* **1982**, *144*, 144.
(28) Andersson, S. L. T. *Catal. Lett.* **1990**, *7*, 351.
(29) Griffith, W.; Lesniak, P. *J. Chem. Soc. A* **1969**, 1066.
(30) Cavani, F.; Centi, G.; Foresti, E.; Trifiro, F.; Busca, G. *J. Chem. Soc., Faraday Trans. 1* **1988**, *84*, 237.
(31) Inomata, M.; Mori, K.; Ui, T.; Miyamoto, A.; Murakami, Y. *J. Phys. Chem*. **1983**, *87*, 754.
(32) Lischke, G.; Hanke, W.; Jerschkewitz, H.; Ohlmann, G. *J. Catal*. **1985**, *91*, 54.
(33) Rajadhyaksha, R.; Hausinger, G.; Zeilinger, H.; Ramstetter, A.; Schmelzand, H.; Knozinger, H. *Appl. Catal*, **1989**, *51*, 67.
(34) Arco, M.; Holgado, M.; Martin, C.; Rives, V. *J. Catal*. **1986**, *99*, 19.
(35) Malet, P.; Munoz-Paez, A.; Martin, C.; Rives, V. *J. Catal*. **1992**, *134*, 47.
(36) Hatayama, F.; Ohno, T.; Maruoka, T.; Ono, T.; Miyata, H. *J. Chem. Soc., Faraday Trans. 1* **1991**, *87*, 2629.
(37) Nieto, L.; Kgemenic, G.; Fierro, J. L. G. *Appl. Catal.* **1990**, *61*, 235.
(38) Handy, B.; Baiker, A.; Schralm-Marth, M.; Wokaun, A. *J. Catal.* **1992**, *133*, 1.
(39) Chan, S.; Wachs, I.; Murrell, L.; Wang, L.; Hall, K. *J. Phys. Chem.* **1984**, *88*, 5831.
(40) Hardcastle, F. D.; Wachs, I. E. *J. Mol. Catal.* **1988**, *46*, 173.
(41) Wachs, I. E.; Saleh, R. Y.; Chan, S. S.; Chersich, C. C. *Appl. Catal*. **1985**, *15*, 339.
(42) Went, G.; Oyama, S.; Bell, A. *J. Phys. Chem*. **1990**, *94*, 4240.
(43) Solar, J.; Basu, P.; Shatlock, M. *Catal. Today* **1992**, *14*, 211.
(44) Deo, G.; Wachs, E. *J. Phys. Chem*. **1991**, *95*, 5889.
(45) Handy, B.; Baiker, A.; Schraml-Marth, M.; Wokaun, A. *J. Catal*. **1992**, *133*, 1.
(46) Ehgweiler, J.; Baiker, A. *Appl. Catal. A: Gen.* **1994**, *120*, 187.
(47) Lietti, L.; Forzatti, P.; Ramis, G.; Busca, G.; Bregani, F. *Appl. Catal. B: Environ.* **1993**, *3*, 13.
(48) Nickl, J.; Dutoit, D.; Baiker, A.; Scharf, U.; Wokaun, A. *Appl. Catal. A: Gen.* **1993**, *98*, 173.
(49) Machej, T.; Haber, J.; Turek, A.; Wachs, I. *Appl. Catal*. **1991**, *70*, 115.
(50) Eckert, H.; Wachs, I. E. *J. Phys. Chem.* **1989**, *93*, 679.
(51) Centi, G.; Pinelli, D.; Trifiro, F.; Ghaussoub, D.; Guelton, M.; Gengembre, L. *J. Catal*. **1991**, *130*, 238.
(52) Centi, G.; Giamello, E.; Pinelli, D.; Trifiro, F. *J. Catal*. **1991**, *130*, 220.
(53) Ciambelli, P.; Bagnasco, G.; Lisi, L.; Turco, M.; Chiarello, G.; Musci, M.; Notaro, M.; Chetti, P. *Appl. Catal: B Environ.* **1992**, *1*, 61.
(54) Bond, G. C.; Zurita, J. P.; Flamerz, S. *Appl. Catal*. **1986**, *27*, 353.
(55) Van Hengtsum, A. J.; Pranger, J.; Van Ommen, J. G.; Gellings, P. J. *Appl. Catal*. **1984**, *11*, 317.
(56) Van Hengstum, A. J.; Van Ommen, J. G.; Bosch, H.; Gellings, P. J. In *Proceedings of the 8th International Congress on Catalysis*; Dechema: Frankfurt-am-Main, 1984; Vol. 4, p 297.
(57) Roozeboom, F.; Mittelmeijer-Hazeleger, M. C.; Moulijn, J. A.; Medema, J.; Beer, V. H. J.; de Jenkins, P. J. *J. Phys. Chem*. **1980**, *84*, 2783.
(58) Bond, G. C.; Perez Zurita, J.; Flamerz, S.; Gellings, P. J.; Bosch, H.; Van Ommen, J. G.; Kip, B. J. *Appl. Catal*. **1986**, *22*, 361.
(59) Georgiadou, I.; Slavov, S.; Papadopoulou, Ch.; Matralis, H. K.; Kordulis, Ch. *Bull. Soc. Chim. Belg.* **1995**, *104*, 143.
(60) Srnak, Z.; Dumesic, T. A.; Clausen, B. S.; Tornquist, E.; Topsoe, N. Y. *J. Catal.* **1992**, *135*, 246.
(61) Topsoe, N. Y. *J. Catal*. **1991**, *128*, 499.
(62) Matralis, H.; Ciardelli, M.; Ruwet, M.; Grange, P. *J. Catal*. **1995**, *157*, 368.
(63) Cavani, F.; Centi, G.; Parrinello, F.; Trifiro, F. T. In *Preparation of Catalysts V*; Delmon, B., Grange, P., Jacobs, P. A., Poncelet, G., Eds.; Elsevier: Amsterdam, 1987; p 227.
(64) Clarebout, G.; Ruwet, M.; Matralis, H.; Grange, P. *Appl. Catal*. **1991**, *76*, L9.